Improved registration of DCE-MR images of the liver using a prior segmentation of the region of interest

Zhang, Tian; Li, Zhang; Runge, Jurgen H.; Lavini, Cristina; Stoker, Jaap; Van Gulik, Thomas; Van Vliet, Lucas J.; Vos, Frans M.

DOI
10.1117/12.2216668

Publication date
2016

Document Version
Final published version

Published in
Medical Imaging 2016: Image Processing

Improved registration of DCE-MR images of the liver using a prior segmentation of the region of interest

Tian Zhang*[a], Zhang Li[b], Jurgen H. Runge[c], Cristina Lavini[c], Jaap Stoker[c], Thomas van Gulik[d], Lucas J. van Vliet[a], Frans M. Vos[a,c]

[a)] Quantitative Imaging Group, Department of Imaging Physics, Delft University of Technology, 2628 CJ, Delft, The Netherlands; [b)] College of Aerospace Science and Engineering, National University of Defense Technology, 410073, Changsha, China; [c)] Department of Radiology, Academic Medical Center Amsterdam, 1105 AZ, Amsterdam, The Netherlands; [d)] Department of Surgery, Academic Medical Center Amsterdam, 1105 AZ, Amsterdam, The Netherlands

ABSTRACT

In Dynamic Contrast-Enhanced MRI (DCE-MRI) of the liver, a series of images is acquired over a period of 20 minutes. Due to the patient's breathing, the liver is subject to a substantial displacement between acquisitions. Furthermore, due to its location in the abdomen, the liver also undergoes marked deformation. The large deformations combined with variation in image contrast make accurate liver registration challenging.

We present a registration framework that incorporates a liver segmentation to improve the registration accuracy. The segmented liver serves as region-of-interest to our in-house developed registration method called ALOST (autocorrelation of local image structure). ALOST is a continuous optimization method that uses local phase features to overcome space-variant intensity distortions. The proposed framework can confine the solution field to the liver and allow for ALOST to obtain a more accurate solution. For the segmentation part, we use a level-set method to delineate the liver in a so-called contrast enhancement map. This map is obtained by computing the difference between the last and registered first volume from the DCE series. Subsequently, we slightly dilate the segmentation, and apply it as the mask to the other DCE-MRI volumes during registration. It is shown that the registration result becomes more accurate compared with the original ALOST approach.

Keywords: Registration, Liver Segmentation, DCE-MRI, ALOST, Level-set

1. INTRODUCTION

Dynamic Contrast-Enhanced MRI (DCE-MRI) is widely used to investigate the functioning of many organs. Important parameters quantifying the capillary permeability can be extracted from the time intensity data using pharmacokinetic models. However, DCE-MRI of the abdomen is hindered by motion due to breathing, and the resulting dynamic images are not aligned to each other. Many algorithms have been proposed to solve similar registration problems, e.g. based on normalized mutual information (NMI)[1] and the modality independent neighborhood descriptor (MIND)[2]. However, the outcome of these general approaches on DCE images can be inaccurate due to large spatial deformations and variations in the image contrast due to the inflow of contrast agent. A registration method called autocorrelation of local image structure metric (ALOST)[3] has been shown to efficiently deal with contrast variations. Still, the problem remains challenging due to the large magnitude of prevalent deformations.

In this paper, the focus is on liver imaging. We introduce an explicit segmentation of the organ into the ALOST technique, in order to emphasize our region of interest during registration. The segmentation is obtained by applying a level-set method to a so-called contrast enhancement map. We will show that the initial segmentation improves the registration precision by restricting the search space.

In this paper we first briefly introduce the registration method ALOST, the liver segmentation method and a model for determining the intracellular uptake rate of the contrast agent. Subsequently, we evaluate the liver mask extraction method and evaluate the registration performance of the proposed framework compared to the original ALOST approach.

Medical Imaging 2016: Image Processing, edited by Martin A. Styner, Elsa D. Angelini, Proc. of SPIE Vol. 9784, 978443 · © 2016 SPIE
CCC code: 1605-7422/16/$18 · doi: 10.1117/12.2216668

2. METHODOLOGY

2.1 Registration by autocorrelation of local image structure (ALOST)

The modality independent neighborhood descriptor (MIND) method[2] is a state-of-the-art registration technique for multi-modal image registration. Essentially, it relies on a patch-based descriptor of the structure in a local neighborhood:

$$MIND\left(I,\mathbf{x},\mathbf{r}\right)=\frac{1}{n}\exp\left(-\frac{D_p\left(I,\mathbf{x},\mathbf{x}+\mathbf{r}\right)}{V\left(I,\mathbf{x}\right)}\right) \tag{1}$$

in which I is an image, $\mathbf{r}$ is an offset in neighborhood R of size $R\times R$ around position $\mathbf{x}$ and n a normalization constant; D_p is the distance between two image patches, measured by the sum of squared differences (SSD):

$$D_p\left(I,\mathbf{x_1},\mathbf{x_2}\right)=\sum_{\mathbf{p}\in P}\left(I\left(\mathbf{x}_1+\mathbf{p}\right)-I\left(\mathbf{x}_2+\mathbf{p}\right)\right)^2 \tag{2}$$

and $V(I, \mathbf{x})$ is the mean of the patch distances in a small neighborhood N:

$$V\left(I,\mathbf{x}\right)=\frac{1}{num\left(N\right)}\sum_{\mathbf{p}\in P}D_p\left(I,\mathbf{x},\mathbf{x}+\mathbf{n}\right) \tag{3}$$

Recently, we have introduced a novel registration metric that relies on the monogenic signal[4]. The monogenic signal is a generalization of the so-called analytic signal from one to higher dimensions based on the Riesz transform. The analytic representation of a signal applies the concept that negative frequency components of a 1-D, real-valued signal are essentially superfluous due to the Hermitian symmetry of the Fourier Spectrum.

The monogenic signal is an efficient tool to describe the local image structure by means of local phase. Particularly, the mean phase (MP), i.e. the average phase calculated over several scales, serves as an identifier for the type of image feature. For example, a step corresponds to $\phi = 0$ and a peak to $\phi = \pi$. Furthermore, it has been recognized that salient features are perceived at points in an image where the Fourier components are in phase. Several measures for phase congruency[5] (PC) have been developed expressing that if all scale components are in phase, PC = 1; alternatively, if there is no coherence of phase, then PC = 0.

The mean phase and phase congruency extracted from the monogenic signal share the same advantage that they are insensitive to space-variant intensity distortions, e.g. the intensity difference due to contrast enhancement and the MRI bias field. This ability is what the MIND approach lacks[3]. Therefore, we have integrated MP and PC into MIND to extract local image information into a descriptor called ALOST[3]:

$$ALOST\left(I,\mathbf{x},\mathbf{r}\right)=\left[MIND\left(MP\left(I\right),\mathbf{x},\mathbf{r}\right),MIND\left(PC\left(I\right),\mathbf{x},\mathbf{r}\right)\right] \tag{4}$$

Essentially, the registration is performed by minimizing the next energy function

$$E\left(\mathbf{w}\right)=E_{ALOST}\left(\mathbf{w}\right)+\alpha E_R\left(\mathbf{w}\right) \tag{5}$$

where α is a weighting coefficient that balances the two terms of our energy function:

1. Data term

$$E_{ALOST}\left(\mathbf{w}\right)=\int_{\Omega}\left[ALOST_m\left(\mathbf{x}+\mathbf{w}\left(\mathbf{x}\right)\right)-ALOST_f\left(\mathbf{x}\right)\right]^2 d\mathbf{x}\ . \tag{6}$$

2. Regularization term

$$E_R(\mathbf{w}) = \int_\Omega \left[\nabla u(\mathbf{x})\right]^2 + \left[\nabla v(\mathbf{x})\right]^2 + \left[\nabla w(\mathbf{x})\right]^2 d\mathbf{x} \ , \tag{7}$$

where $\mathbf{w} = [u,v,w]$ is the 3D deformation field. More details on the ALOST approach can be found in [3].

In our DCE-MRI scan, the total imaging time was approximately 20 minutes (more details are given below). During imaging, we let the patient hold his/her breath, especially around the time when the contrast agent arrived in the liver. We did this to limit images distortion by intra-scan motion, as these images are crucial for accurate pharmacokinetic imaging. However, we have observed that these images show large distortions compared to images acquired during regular breathing, i.e. acquired at the beginning and the end of the DCE series.

As ALOST could not cope with such distortion, we restrict the search space of the registration by suing a prior segmentation of the liver as a region of interest.

2.2 Segmentation

The liver shows the strongest contrast enhancement at the end of the DCE series. This is generally termed the hepatic phase, as the uptake rate of the contrast agent into the liver cells reaches its maximum at that time. Accordingly, subtraction of the registered first volume from the last volume yields an image in which the liver is maximally "enhanced", whereas other organs are suppressed:

$$CE_{liver} = I_{post} - I_{pre} \ . \tag{8}$$

Notice that the shape and location of the liver are more or less the same in the two images since the patient is breathing rather shallowly at the very beginning and at the end of the DCE series. Therefore, good registration accuracy can be achieved by applying ALOST even without a mask.

In the CE_{liver} map, the liver is very clearly visible (e.g. Figure 2(d)). We use a level-set method to segment the liver in order to obtain the mask. Among several level-set methods, the geodesic[6] and the Chan-Vese[7] models are the benchmarks with respect to boundary- and region-based methods. The hybrid method proposed by Y. Zhang et al.[8] takes boundary as well as region information into consideration while minimizing the next data term:

$$E(\phi) = -\int_\Omega (I-\mu) H(\phi)\, d\Omega + \beta \int_\Omega g \left|\nabla H(\phi)\right| d\Omega \tag{9}$$

where I is the image, g represents the gradient of the image, β is a weighting coefficient, $H(\phi)$ is the Heaviside function, and μ is a parameter that represents the lower bound of the gray-level in the segmented object. Essentially, the first term integrates the (negated) intensity inside the segmented region and the second term integrates the derivative along the boundary of the segmented region.

When the liver mask M_{liver} has been extracted, we dilate it somewhat ($M_{liver}^{dilated}$) to make sure that the liver boundary is included in the mask in most images.

In summary, our approach reduces to the following steps: (1) we register the first volume to the last one, and calculate the contrast enhancement via (8); (2) we segment the liver in the CE_{liver} map and obtain the mask; (3) we dilate the mask somewhat, so that the boundary of the liver is included in the mask (i.e. the most salient information); (4) we apply the dilated mask to the entire image series, while optimizing equation (5). As such, equation (5) is only evaluated over the a priori segmented region. We do so while registering the entire DCE series to the last image since that image shows the largest contrast and has been acquired during shallow breathing.

2.3 Modeled signal in the liver

In order to evaluate the benefit of our approach we will fit a model to the time-intensity signal in the segmented region. The residual of the fit will be considered a measure of the registration accuracy. Therefore, we adopt the liver model proposed by S. Sourbron et al.[9], henceforth referred to as "the Sourbron model". This dual-inlets two-compartment uptake model was especially designed for the intracellular hepatobiliary contrast agent **Gadoxetate disodium** (Primovist™ , Bayer pharmaceutical). The diagram in Figure 1 sketches the model. The arterial input function (AIF) and venous input function (VIF) are the dual inlets since blood is supplied to the liver by the hepatic artery as well as the portal vein. The AIF and VIF represent the contrast agent concentration in the blood plasma of the hepatic artery and

portal vein respectively. These were obtained by averaging the top three time intensity curves having the highest contrast enhancement measured voxel-wise in regions manually delineated in the aorta (cranially from the hepatic artery) and the portal vein. T_A and T_V represent time delays and F_A and F_V are constants representing the volume transfer rates from the plasma compartments into the extravascular, extracellular space. Furthermore, in the gray rectangle denoting liver tissue, the left circle represents the extravascular, extracellular compartment and the right circle stands for the extravascular intracellular compartment, i.e. corresponding to the hepatocytes. As such, V_E is the extravascular, extracellular volume and K_I represents the uptake rate of the hepatocytes represented by a volume V_I.

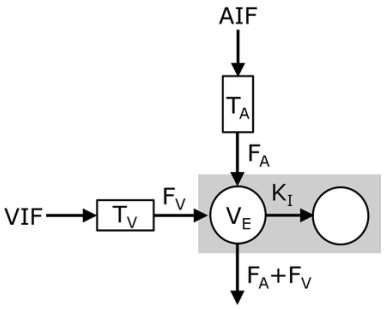

Figure 1. The Sourbron model: a dual-inlets two-compartment uptake model for Primovist in the liver. The AIF and VIF are dual inlets into the liver, representing the concentration of the contrast agent over time entering from the hepatic artery and the portal vein. T_A and T_V are time delays. F_A and F_V are the arterial and venous plasma flows, respectively (in milliliters per minute per 100 mL). In the gray rectangle representing the liver, the left circle represents the extravascular extracellular compartment V_E (in milliliters per 100 mL) and the right circle stands for the hepatocyte compartment. K_I (per minute) is the liver uptake rate.

Let C_E and C_I be the contrast agent concentrations in the extravascular, extracellular compartment and hepatocytes, respectively. Defining C_A and C_V as the concentrations of the AIF and VIF, the mass transport between the two compartments can be expressed as

$$\begin{cases} V_E \dfrac{dC_E}{dt}(t) = F_A C_A(t - T_A) + F_V C_V(t - T_V) - (F_A + F_V + K_I) C_E(t) \\ V_I \dfrac{dC_I}{dt}(t) = K_I C_E(t) \end{cases} \tag{10}$$

and the solution for the total liver tissue concentration ($C_T = V_E C_E + V_I C_I$) is

$$C_T(t) = \left[T_E \delta(t) + \frac{K_I}{F_A + F_V + K_I} \right] * \frac{e^{-\frac{t}{T_E}}}{T_E} * \left[F_A C_A(t - T_A) + F_V C_V(t - T_V) \right] \tag{11}$$

where * is the convolution operator.

3. RESULTS

DCE-MRI data were acquired from 8 patients on a 3T Philips scanner via a 3D SPGR sequence. The acquisition parameter settings were TE/TR = 2.3/3.75 ms, FA = 15°, matrix size = 128×128×44, voxel size = 3×3×5 mm^3, acquisition time = 2.141 s for each volume; the sampling interval (between images) was 2.141 s for volumes 1-81, 30 s for volumes 82-98 and 60 s for volumes 99-108. The total imaging time was approximately 20 minutes. Patients held their breath during the acquisition of volumes 13-22, 33-42, 61-70 and 79-108.

Exemplary pre-contrast and post-contrast images are shown in Figure 2 (a) and (b), respectively. Obviously, the liver is highly enhanced in the post-contrast image. Figure 2(c) is the outcome of registering (a) to (b) by ALOST without applying a mask. Actually, in (a) and (c) the location and shape of the liver are almost the same since the patients breathed quietly at the very beginning and at the end of the acquisition series. Figure 2(d) is the CE_{liver} map, which is calculated by (8). In this image, the liver is highlighted while the other organs in the abdomen display a very low intensity.

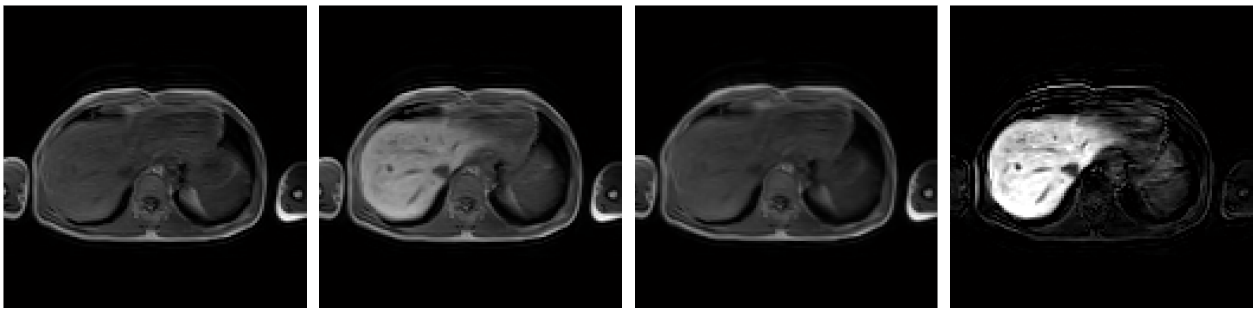

(a) (b) (c) (d)

Figure 2. (a) Pre-contrast image (the first volume); (b) post-contrast image (the last volume); (c) the registered image of (a) by ALOST without liver mask; (d) the CE_{liver} map

Figure 3 and Figure 4 show the 3D liver mask (i.e. the segmentation) and 2D cross-sections of the mask boundary overlaid on the CE_{liver} map. Clearly, the mask matches the liver very well.

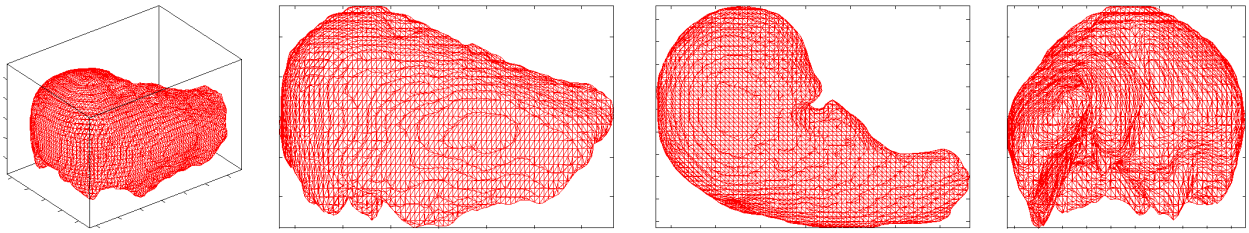

(a) (b) (c) (d)

Figure 3. 3D mask (segmentation) of the liver. (a) 3D view; (b) the front view; (c) the top view; (d) the right side view.

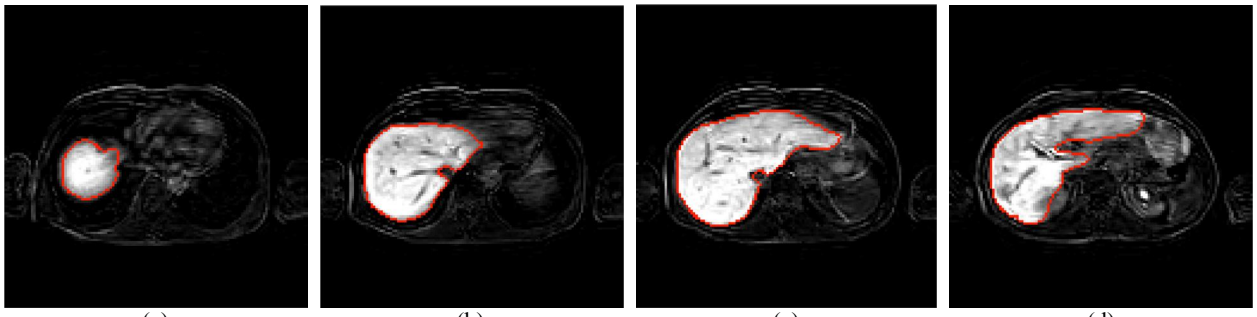

(a) (b) (c) (d)

Figure 4. Overlay of CE_{liver} map and the liver mask's boundary. (a) slice 36; (b) slice 31; (c) slice 27; (d) slice 21.

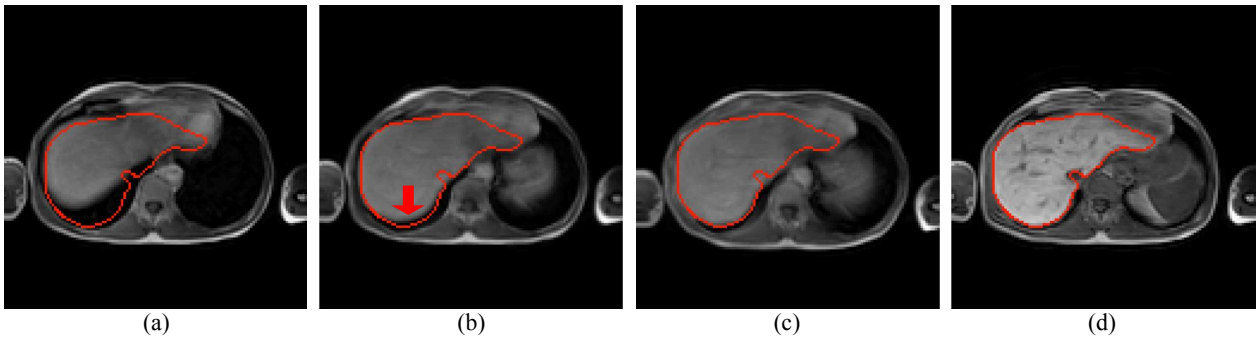

(a) (b) (c) (d)

Figure 5. (a) moving image; (b) registered image by ALOST alone; (c) registered image by ALOST supported by the dilated liver mask; (d) fixed image

The registration improvement by application of a mask is illustrated in Figure 5. The moving image and the fixed image are shown in Figure 5(a) and (d), respectively. We also drew the outline of the liver mask in figure (d) and copied it to the other sub figures to facilitate the comparison. The registration result obtained by ALOST alone can be seen in Figure 5(b). Compared with the moving image, the liver in Figure 5(b) is more similar to Figure 5(d), but near the bottom of the liver mask, the mismatch, indicated by the red arrow, shows that the registration is still off. Figure 5(c) shows that ALOST supported by the dilated liver mask produces a more accurate registration outcome.

Furthermore, we chose another slice and selected a line segment through the liver to investigate the intensity as a function of time, see Figure 6(a). In Figure 6 (b)-(d) the edge of the dilated liver mask is also drawn for reference. Large fluctuations can be observed over time along this line prior to registration, see Figure 6(b). Most of the fluctuations are compensated by ALOST, see Figure 6(c), but some mismatches are still visible. The most accurate outcome is generated by ALOST supported by the dilated liver mask, as demonstrated in Figure 6(d).

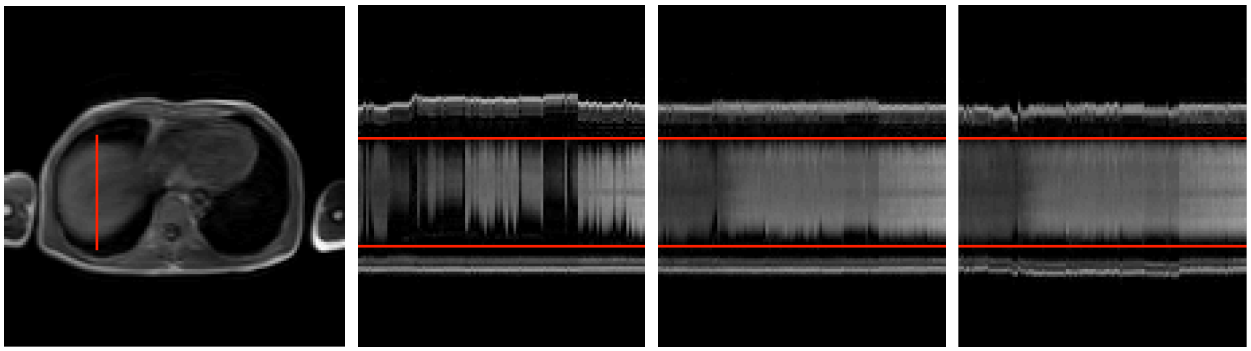

(a) (b) (c) (d)

Figure 6. (a) Transverse plane of slice 34. (b)-(d) Intensity as a function of time along the red line: (b) raw DCE data (prior to registration); (c) ALOST registration without the dilated liver mask; (d) ALOST registration with the dilated liver mask.

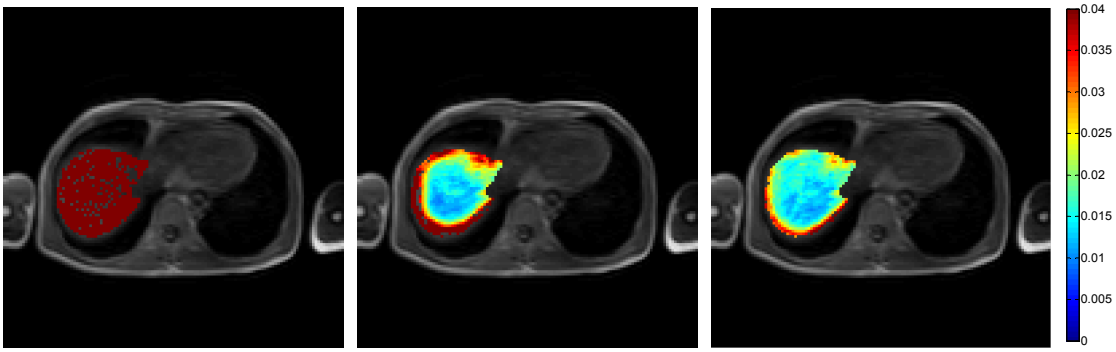

(a) (b) (c)

Figure 7. RMSE of fitting the liver model function to the intensity data from each pixel: (a) raw DCE data; (b) ALOST data without the dilated liver mask; (c) ALOST data with the dilated liver mask.

Figure 7 shows the distribution of the root mean square error (RMSE) that remains after fitting the Sourbron model to the time intensity curves (TICs). One can see that the RMSE is huge when no registration is performed, see Figure 7(a). In Figure 7(b), produced by ALOST registration without the liver mask, the RMSE is only large near the boundary of the liver, where there is large fluctuation in signal intensity due to mis-registration. The smallest RMSE is provided by ALOST registration supported by the dilated liver mask, see Figure 7(c). Notice that the RMSE is especially reduced near the edge of the liver.

Henceforth, we focus on investigating the registration performance near the liver boundary. Therefore, the liver mask was eroded by a 26-connected 3x3x3 kernel and then subtracted from the original liver mask. As a result, a mask is

obtained of the liver boundary. Figure 8 shows how the RMSE measure varies at the boundary of liver in the first patient prior to registration and after registration without and with support of the dilated liver mask.

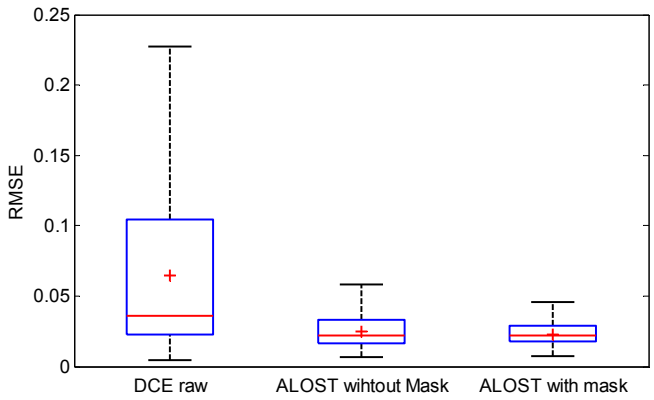

Figure 8. Box-and-whisker plots of the root mean squared error (RMSE) of the model fits at the liver boundary prior to registration (DCE raw) and after registration without and with support of the dilated liver mask.

Table 1. Evaluation of the registration performance on 8 abdominal DCE-MRI datasets by ALOST without and with the support of the dilated liver mask. The performance was measured by the RMSE that remains after fitting the Sourbron model to TICs near the liver boundary. The numbers report the mean value and the standard deviation (std) between brackets. The numbers printed in boldface are the best result per row.

	DCE raw	**ALOST without Mask**	**ALOST with Mask**
Patient 1	0.0643 (0.0607)	0.0248 (0.0116)	**0.0228 (0.0075)**
Patient 2	0.0361 (0.0254)	0.0230 (0.0114)	**0.0215 (0.0083)**
Patient 3	0.0326 (0.0191)	0.0289 (0.0163)	**0.0282 (0.0141)**
Patient 4	0.0570 (0.0352)	0.0518 (0.0263)	**0.0484 (0.0214)**
Patient 5	0.0366 (0.0171)	0.0289 (0.0139)	**0.0276 (0.0116)**
Patient 6	0.0676 (0.0557)	0.0367 (0.0191)	**0.0313 (0.0132)**
Patient 7	0.0445 (0.0317)	0.0299 (0.0178)	**0.0272 (0.0129)**
Patient 8	0.0573 (0.0444)	0.0324 (0.0186)	**0.0302 (0.0141)**

Figure 8 shows the distribution of the RMSE at the liver boundary. Apparently, ALOST with support of the dilated liver mask achieves the smallest RMSE value and standard deviation. The same approach applied to all 8 patients yields the outcomes shown in table 1. It demonstrates that ALOST with support of the dilated liver mask achieves the best registration accuracy.

4. CONCLUSION

The framework proposed by us integrates a liver segmentation into the ALOST registration framework. This segmentation method was based on the so-called contrast enhancement map. The prior segmentation supports ALOST by restricting the search space. The improved registration was demonstrated by better fits of the Sourbron model to the time intensity data after registration. The proposed framework can be easily adapted to other DCE-MRI applications with different contrast agents provided that a segmentation of the organ of interest is available.

REFERENCES

[1] Studholme, C., Hill, D. L. G.., Hawkes, D. J., "An overlap invariant entropy measure of 3D medical image alignment," Pattern Recognit. 32(1), 71–86 (1999).

[2] Heinrich, M. P., Jenkinson, M., Bhushan, M., Matin, T., Gleeson, F. V., Brady, S. M.., Schnabel, J. A., "MIND: Modality independent neighbourhood descriptor for multi-modal deformable registration," Med. Image Anal. 16(7), 1423–1435 (2012).

[3] Li, Z., Mahapatra, D., Tielbeek, J., Stoker, J., van Vliet, L.., Vos, F., "Image registration based on autocorrelation of local structure," IEEE Trans. Med. Imaging 62(99), 1–13 (2015).

[4] Felsberg, M.., Sommer, G., "The monogenic signal," IEEE Trans. Signal Process. 49(12), 3136–3144 (2001).

[5] Kovesi, P., "Edges Are Not Just Steps," ACCV2002 5th Asian Conf. Comput. Vis.(January), 23–25 (2002).

[6] Caselles, V., Kimmel, R.., Sapiro, G., "Geodesic Active Contours," Int. J. Comput. Vis. 22(1), 61–79 (1997).

[7] Chan, T. F.., Vese, L. a., "Active contours without edges.," IEEE Trans. Image Process. 10(2), 266–277 (2001).

[8] Zhang, Y., Matuszewski, B. J., Shark, L.-K.., Moore, C. J., "Medical Image Segmentation Using New Hybrid Level-Set Method," 2008 Fifth Int. Conf. Biomed. Vis. Inf. Vis. Med. Biomed. Informatics, 71–76 (2008).

[9] Sourbron, S., Sommer, W. H., Reiser, M. F.., Zech, C. J., "Combined Quantification of Liver Perfusion and Function with Dynamic Gadoxetic Acid-enhanced MR Imaging," Radiology 263(3), 874–883 (2012).